OncoTargets and Therapy

Dovepress
open access to scientific and medical research

Open Access Full Text Article

ORIGINAL RESEARCH

miR-495-3p inhibits the cell proliferation, invasion and migration of osteosarcoma by targeting C1q/TNF-related protein 3

This article was published in the following Dove Press journal:
OncoTargets and Therapy

Gang Zhao[1]
Liwei Zhang[2]
Dejian Qian[1]
Yifeng Sun[1]
Wei Liu[1]

[1]Orthopaedics Department, Shandong Provincial Qianfoshan Hospital, Shandong University, Jinan, Shandong 250014, People's Republic of China; [2]Burn and Plastic Surgery Department, Juye County North City Hospital, He Ze, Shandong 274900, People's Republic of China

Background: Osteosarcoma (OS) is one of the most common malignant tumors of bone, and microRNAs (miRNAs/miRs) serve critical roles in the progression of human OS. The aim of the present study was to investigate the role of miR-495-3p in OS.

Methods: The expression of miR-495-3p in OS tissues and adjacent tissues from 30 patients was measured by reverse transcription-quantitative PCR (RT-qPCR). Human OS cell lines (U-2 OS, MG-63 and Saos-2 cells) and normal osteoplastic cells (hFoB 1.19 cells) were employed to perform the further analysis. The cell proliferation ability of MG-63 cells was measured by Cell Counting Kit-8 assay and colony formation assay. In addition, cell invasion and migration were evaluated by Transwell and scratch wound healing assays, respectively. Flow cytometry was applied to assess cell apoptosis and the cell cycle. Moreover, RT-qPCR and Western blotting were performed to measure mRNA and protein expression. A luciferase reporter assay was used to verify the target gene of miR-495-3p. Furthermore, a xenograft OS model was made to evaluate the effect of miR-495-3p in vivo.

Results: The results revealed that miR-495-3p was downregulated in the OS tissues and GBM cell lines. Additionally, miR-495-3p overexpression suppressed the proliferation, migration and invasion of MG-63 cells. Simultaneously, cell apoptosis was promoted, accompanied by cell cycle arrest, after transfecting with miR-495-3p mimics. In addition, the expression levels of cell apoptosis-related proteins were increased, whereas proteins of the cell cycle were decreased. Importantly, C1q/TNF-related protein 3 (CTRP3) was confirmed as a direct target of miR-495-3p. A xenograft tumor model was employed to verify the effects of miR-495-3p on OS.

Conclusion: On the basis of these results, we conclude that miR-495-3p overexpression inhibited cell proliferation, migration and invasion by downregulating CTRP3. Therefore, miR-495-3p may act as a tumor suppressor and an underlying target for OS treatment.

Keywords: osteosarcoma, miR-495-3p, invasion, C1q/TNF-related protein 3

Introduction

Osteosarcoma (OS) is a malignant bone tumor that is characterized by its marked aggression and rapid progression, and is becoming a leading cause of cancer death in children and young adults.[1,2] Despite the rapid development of OS therapeutic strategies involving surgery combined with chemotherapy, the 5-year survival rate of patients is still unsatisfactory, which is attributed to the high invasiveness of the disease and poor responses to treatment.[3,4] Therefore, there is an urgent need to ascertain new avenues to effectively target and treat OS and improve the clinical survival rate of OS patients.

Correspondence: Wei Liu
Orthopaedics Department, Shandong Provincial Qianfoshan Hospital, Shandong University, Jingshi Road 16766, Jinan, Shandong 250014, People's Republic of China
Email liuweihyc@163.com

submit your manuscript | www.dovepress.com
DovePress
http://doi.org/10.2147/OTT.S193937

MicroRNAs (miRNA/miRs) are a class of small non-coding RNAs of 19–24 nucleotides in length which exert significantly regulatory effects in gene expression.[5,6] It has been well documented in recent decades that miRNAs are implicated in the initiation and progression of cancer.[7–9] Furthermore, miRNAs play crucial roles in regulating multiple processes in OS occurrence and development, such as proliferation, apoptosis, invasion, migration and metastasis.[10,11] It has been reported that miR-495-3p may have an oncogenic or anticancer effect in several cancers. For instance, miR-495-3p inhibits proliferation and invasion in clear cell renal cell carcinoma cells.[12] miR-495-3p serves as a tumor suppressor by regulating multiple epigenetic modifiers in gastric carcinogenesis.[13] In addition, miR-495-3p promotes colon cancer cell proliferation via the Wnt/β-catenin signaling pathway.[14] However, the role of miR-495-3p in OS remains to be elucidated.

C1q/TNF-related protein 3 (CTRP3), a new adipokine, plays important roles in multiple physiological processes, including lowering glucose levels, suppressing gluconeogenesis in the liver, and decreasing inflammation.[15–17] Emerging evidence supports the notion that CTRP3 is implicated in bone metabolism due to its negative regulation of osteoclastogenesis.[18] Moreover, a recent study reported that the serum CTRP3 level is associated with osteoporosis in postmenopausal women.[19] Taken together, all of these previous studies drew our attention to the role of CTRP3 in OS.

As an attempt to develop an alternative and effective therapy, we have explored the effect and underlying molecular mechanism of miR-495-3p in OS in the present study. We found that the expression of miR-495-3p was notably decreased in OS tissues and cell lines. miR-495-3p overexpression impeded proliferation, migration and invasion, and promoted apoptosis in OS cells. Moreover, we found that CTRP3 was a direct target of miR-495-3p. In vivo, miR-495-3p overexpression suppressed tumor growth in OS by reducing CTRP3 expression. Collectively, our study revealed that miR-495-3p may act as a tumor suppressor and an underlying target for OS treatment.

Materials and methods

Patient samples

A total of 30 pairs of OS samples and matched adjacent normal samples were collected from patients who underwent surgery at Qianfoshan Hospital between March 2017 and February 2018. Those patients consisted of 17 males and 13 females whose age ranged from 10 to 60 years, with an average age of 30±7.4 years. All patients received surgical resection, and cancer tissues and adjacent normal tissues within 0.5 cm around the tumors were collected during surgery. All samples were placed immediately into liquid nitrogen after surgery. Analysis of the extent of the primary tumor was performed according to the criteria established by American Cancer Society. There were 7 cases at T1, 13 cases at T2 and 10 cases at T3 stage. At the same time, 30 healthy controls with similar age and gender distributions were recruited to serve as a control group. This study was approved by the Ethics Committee of Qianfoshan Hospital, Shandong University, and all adult patients and a parent for patients under 18 years of age provided written informed consent. All of the procedures were performed in accordance with the Declaration of Helsinki and relevant policies in China.

Cell culture

The human OS cell lines (U-2 OS, MG-63 and Saos-2) and the normal human osteoplastic cell line (hFoB 1.19) were purchased from the Cell Bank of the Chinese Academy of Sciences (Shanghai, China), and cultured in Dulbecco's modified Eagle's medium (DMEM) supplemented with 10% fetal bovine serum (FBS). Cells were incubated in a humidified chamber with 5% CO_2 at 37 °C.

Cell transfection

MG-63 cells were seeded into 6-well plates, and transfected with mimic control (miR-NC) or miR-495-3p mimic (Shanghai GenePharma Co., Ltd., Shanghai, China) at a concentration of 40 nM using Lipofectamine® 2000 reagent (Invitrogen, CaliforniaThermo Fisher Scientific, Waltham, MA, USA) when they reached 60–70% confluence.

Cell viability assay

MG-63 cells were seeded into 96-well plates (1×10^4) and cultured for 48 h after transfection. Cell viability was determined using a Cell Counting Kit-8 assay (CCK-8; Shanghai Yi Sheng Biotechnology Co., Ltd., Shanghai, China) according to the manufacturer's instructions. At 48 h after transfection, 10 µl CCK-8 reagent was added to each well and incubated at 37 °C and 5% CO_2 for 4 h. The optical density (OD) value was measured at 450 nm on a microplate reader. Each experiment was performed in triplicate.

Colony formation assay

MG-63 cells were seeded into 6-well plates (500 cells/well) and cultured at 37 °C and 5% CO_2 for 7–12 days. The cells

were fixed and stained with 0.2% crystal violet. Colony numbers were counted manually using Image J software.

Cell migration assay

The migratory ability of MG-63 cells was detected by scratch wound healing assay. Cells were seeded into 6-well plates (5×10^3 cells/well) for 24 h. The monolayers were scratched using a 200 µl pipette tip and then the floating cells were removed by washing with PBS. Subsequently, the cells were incubated in serum-free DMEM for 48 h and photographed with a camera connected to a microscope. The percentage wound healing was analyzed using ImageJ software.

Cell invasion assay

Cell invasion was detected by Transwell assay, which was performed in 24-well Transwell plates (Corning Incoporated, Corning, NY, USA) with 8 µm-pore inserts coated with Matrigel (BD Biosciences, San Jose, CA, USA). MG-63 cells in serum-free DMEM were seeded into the upper chamber, while DMEM supplemented with 10% FBS was added to the lower chamber. After 48 h incubation, the Matrigel and the cells remaining in the upper chamber were removed with a cotton-tipped swab. Then, the cells were stained with 1% crystal violet. The number of invasive cells in five random fields (×200) was counted under a light microscope (Olympus Corporation, Tokyo, Japan).

Cell cycle assay

MG-63 cells were seeded into 6-well plates ($5x10^5$) overnight at 37 °C and 5% CO_2. Cell apoptosis was determined using a Cell Cycle Detection kit (KeyGEN BioTECH, Nanjing, China) according to the manufacturer's instructions, and analyzed with FlowJo software (BD Biosciences).

Cell apoptosis assay

MG-63 cells were seeded into 6-well plates (5×10^5) overnight at 37 °C and 5% CO_2. Cell apoptosis was determined using an Annexin V-PE/7AAD Staining Cell Apoptosis Detection kit (KeyGEN BioTECH) according to the manufacturer's instructions, and was analyzed with FlowJo software (BD Biosciences).

Reverse transcription-quantitative PCR (RT-qPCR)

The total RNA was extracted from cells using TRIzol® reagent (Thermo Fisher Scientific). Then, cDNA was synthesized using a RevertAid First Strand cDNA Synthesis kit (K1622; Thermo Fermentas, Waltham, MA, USA) according to the manufacturer's instructions. RT-qPCR was performed using iTaq™ Universal SYBR® Green Supermix (Bio-Rad, Hercules, USA). The sequences of miR-495-3p was 5′-AAACAAACAUGGUGCACUUCUU-3′. The primers used were as follows: CTRP3, forward 5′-TACCTTATGCACAATGGCAACA-3′, reverse 5′-AGCATGATTGCTGGATGTATCTG-3′; miR-495-3p, forward 5′-ACACTCCAGCTGGGAAACAAACATGGTGCA-3′, reverse 5′-TGGTGTCGTGGAGTCG-3′; GAPDH, forward 5′-GGAGCGAGATCCCTCCAAAAT-3′, reverse 5′-GGCTGTTGTCATACTTCTCATGG-3′; U6, forward 5′-CTCGCTTCGGCAGCACA-3′, reverse 5′-AACGCTTCACGAATTTGCGT-3′. GAPDH or U6 was used as an internal control. CTRP3 expression was analyzed using the $2^{-\Delta\Delta Ct}$.

Western blotting analysis

MG-63 cells were harvested and lysed on ice in RIPA Lysis Buffer (Beyotime, Shanghai, China) containing 1mM phenylmethanesulfonyl fluoride (PMSF). The concentration of the proteins was determined using Enhanced BCA Protein Assay kit (Beyotime) according to the manufacturer's instructions. Equal amounts of protein samples were isolated by SDS-PAGE, and subsequently electrophoretically transferred onto polyvinylidene fluoride (PVDF) membranes (EMD Millipore, Billerica, MA, USA). The membranes were blocked with 5% non-fat milk at room temperature for 1 h, and then incubated with primary antibodies (CTRP, 1:1,000, sc-81943; Bcl-2, 1:1,000, sc-509; Bax, 1:1,000, sc-20067; Caspase-3, 1:1,000, sc-271759; p-Rb, 1:1,000, sc-135776; CDK4, 1:1,000, sc-70832; CDK6, 1:1,000, sc-7961; Cyclin D1, 1:1,000, sc-70899; Cyclin A1, 1:1,000, sc-56301; GAPDH, 1:1,000, sc-293335; Santa Cruz Biotechnology Inc., Dallas, TX, USA) overnight at 4 °C. Then, the membranes were washed with TBST three times and incubated with HRP-labeled Goat Anti-Mouse IgG (H+L) antibody (A0216, 1:2,000; Beyotime) at room temperature for 2 h. The blots were developed with an enhanced chemiluminescence (ECL) reagent and analyzed with ImageJ software.

Xenograft tumor model

8-week-old specific-pathogen-free (SPF) nude mice were maintained under pathogen free conditions, and were manipulated in accordance with the ethical guidelines provided under the protocols approved by the Experimental Animal Care Commission at Shandong University. In

addition, the Animal Experimental Ethics Committee of Shandong University approved the experiment. The approval number is no. 2017S055. All of the procedures were performed in accordance with the Declaration of Helsinki and relevant policies in China. Approximately 5.0×10^6 MG-63 cells transfected with miR-495-3p or miR-NC were injected subcutaneously into the right side of the posterior flanks of nude mice. Tumor growth was examined every two days with a vernier caliper. Tumor volumes were calculated using the equation: V ¼ a*b^2/2 (mm^3), where a is the largest diameter, and b is the perpendicular diameter. 21 days after inoculation, all mice were sacrificed and the tumor tissues were weighed. Then, these tissues were employed to perform RT-qPCR and western blot analysis.

Luciferase assay

The target genes of miR-495-3p were predicted using the TargetScan database, version 7.1 (http://www.targetscan.org/vert_71/). Wild-type (WT) and mutant-type (MUT) CTRP 3′-UTR luciferase reporter vectors were designed. miR-495-3p mimics or control were co-transfected with the constructed WT or MUT luciferase reporter vector into MG-63 cells using Lipofectamine 2000. Luciferase activity was assayed using a Dual Luciferase Reporter Gene Assay kit (RG027; Beyotime) after cell transfection for 48 h.

Statistical analysis

All experiments were performed with at least three replicates and all the data are presented as mean±SD. Statistical analysis was performed by SPSS software 16.0. Statistical comparisons were made by one-way ANOVA followed by a post hoc Dunnett's test. A value of $P<0.05$ was considered statistically significant.

Results

The expression of miR-495-3p was significantly downregulated in both OS tissues and cell lines

To evaluate the role of miR-495-3p in OS, the expression level of miR-495-3p in the OS tissues of patients and OS cell lines was measured by RT-qPCR. The results demonstrated that the expression of miR-495-3p was notably downregulated in both OS tissues and cell lines (U-2 OS, MG-63 and Saos-2) compared with adjacent tissues and normal human osteoplastic cells (hFoB 1.19), respectively (Figure 1A and B). To investigate whether miR-495-3p serves as a tumor suppressor in OS, miR-495-3p mimics or negative control was transfected to MG-63 cells. As presented in Figure 1C, overexpression of miR-495-3p was successfully established. These data indicated that decreasing expression of miR-495-3p was correlated with worse progression of OS.

Overexpression of miR-495-3p inhibited the proliferation of OS cells

To explore the effect of miR-495-3p in OS cell proliferation, a CCK-8 assay was used. As presented in Figure 2A and B, overexpression of miR-495-3p markedly suppressed MG-63 cell proliferation compared with the negative control group. In addition, to further confirm the inhibitory effect of miR-495-3p overexpression on the growth of OS cells, a colony formation assay was performed with MG-63 cells (Figure 2C). The

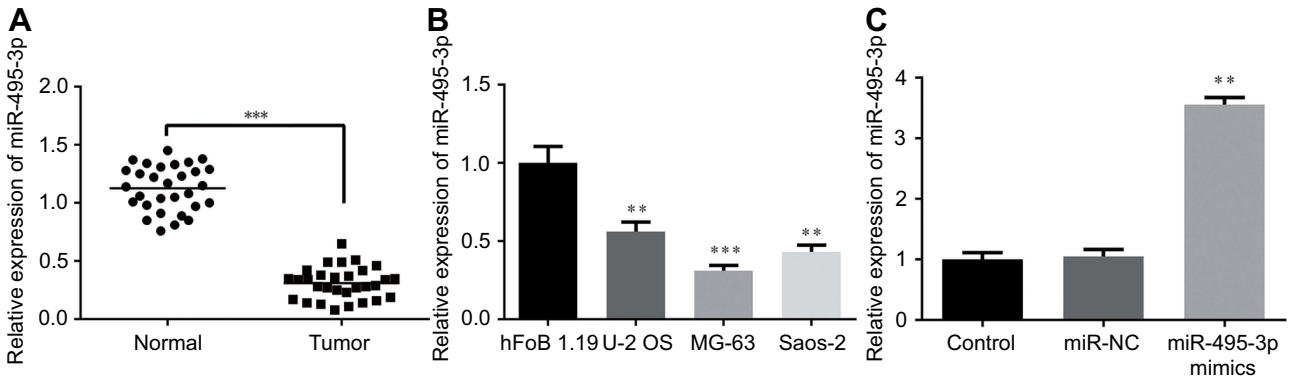

Figure 1 The expression level of miR-495-3p measured by RT-qPCR. (**A**) The expression level of miR-495-3p in OS tissues. ***$P<0.001$ vs normal. (**B**) The expression level of miR-495-3p in human OS cell lines (U-2 OS, MG-63 and Saos-2) and a normal human osteoplastic cell line (hFoB 1.19). **$P<0.01$, ***$P<0.001$ vs hFoB 1.19. (**C**) The expression level of miR-495-3p following miR-495-3p over expression in MG-63 cells. **$P<0.01$ vs miR-NC.

Abbreviations: OS, osteosarcoma; RT-qPCR, reverse transcription-quantitative PCR.

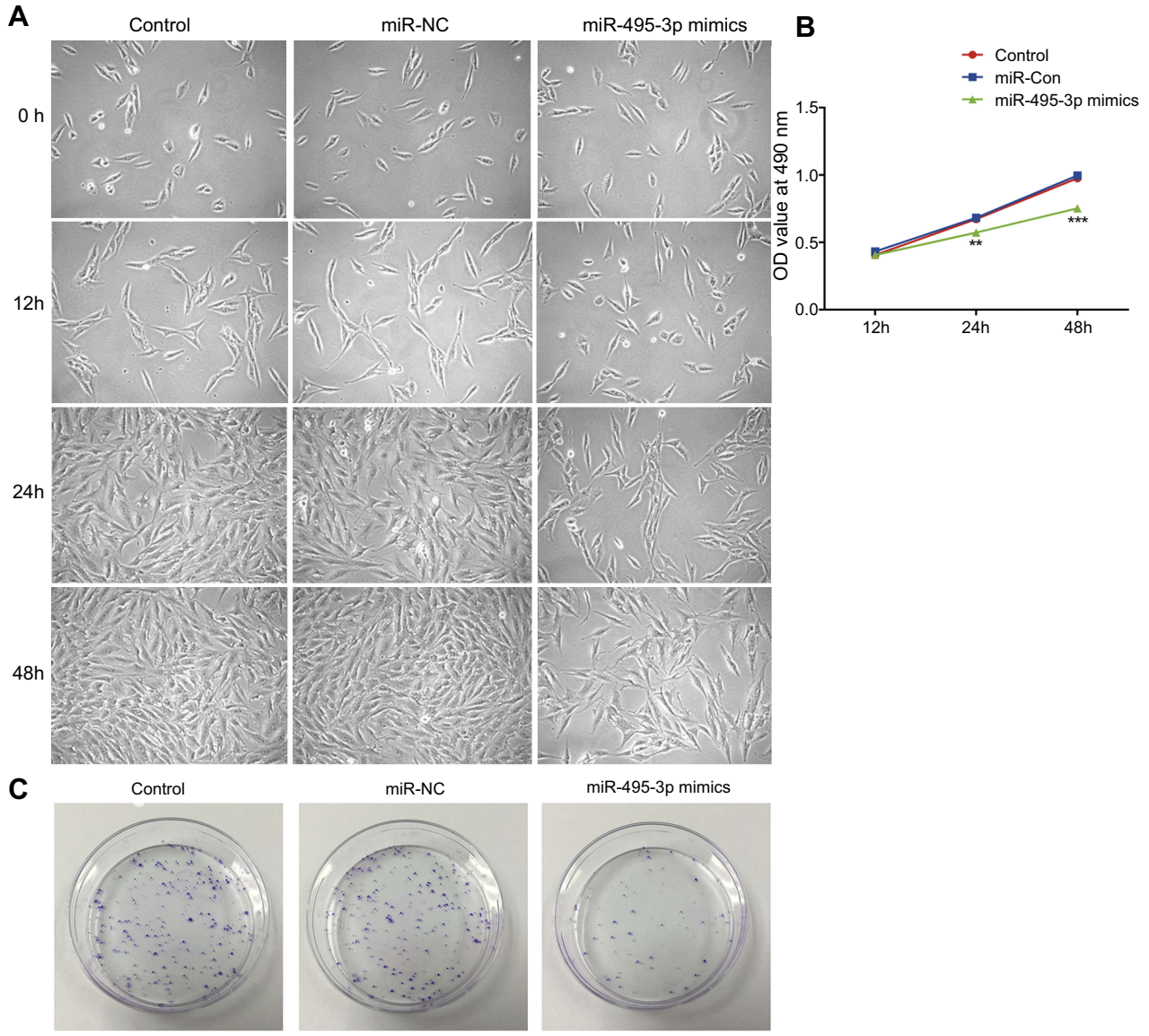

Figure 2 Overexpression of miR-495-3p inhibited the proliferation of MG-63 cells. (**A**) Cell proliferation was detected by an inverted microscope (magnification ×4). (**B**) Cell proliferation was assessed by a Cell Counting Kit-8 assay. $^{**}P<0.01$, $^{***}P<0.001$ vs miR-NC. (**C**) Cell proliferation was measured by colony formation assay.

results illustrated that highly expressed miR-495-3p significantly decreased the colony number of the OS cells, which was in accordance with the CCK-8 assay. The above results suggested that miR-495-3p overexpression was able to inhibit the proliferation of MG-63 cells.

Overexpression of miR-495-3p impeded the invasion and migration of OS cells

Invasion and migration are two key phases involved in OS metastasis. To study the effects of miR-495-3p on the invasion and migration of OS cells, a scratch wound healing assay and a Transwell assay were performed. From the results, we found that the number of invasive and migratory OS cells in the miR-495-3p mimics group was decreased notably compared with the miR-NC group (Figure 3A–D). These results indicated that miR-495-3p overexpression inhibited the invasion and migration of OS cells.

Overexpression of miR-495-3p induced cell cycle arrest as well as promoting the apoptosis of OS cells

The cell cycle and apoptosis following miR-495-3p overexpression were evaluated using flow cytometry in our study. As displayed in Figure 4, the percentages of cells in the G0/G1 phase were increased after miR-495-3p overexpression,

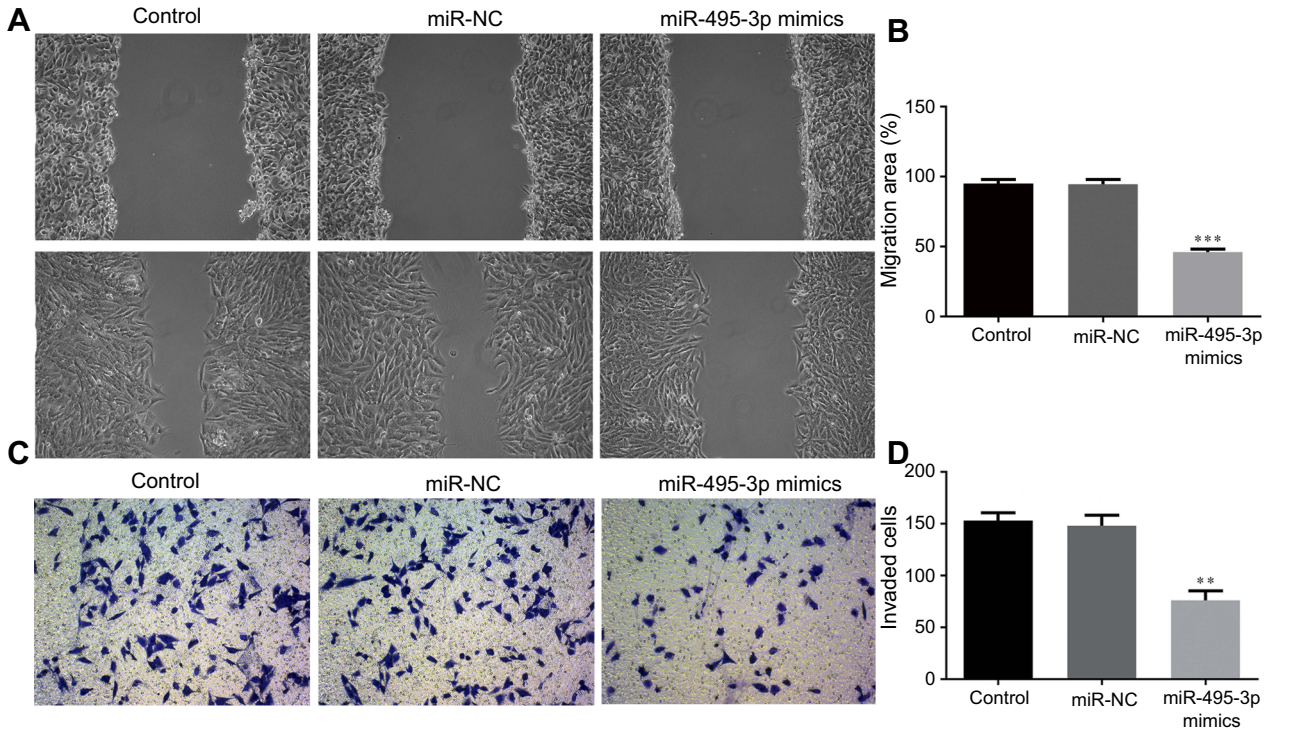

Figure 3 Overexpression of miR-495-3p inhibited the migration and invasion of MG-63 cells. (**A** and **B**) The migratory activity of MG-63 cells was identified with a scratch assay. (**C** and **D**) Cell invasion was assessed with a Transwell assay. ***P*<0.01, ****P*<0.001 vs miR-NC (magnification ×4).

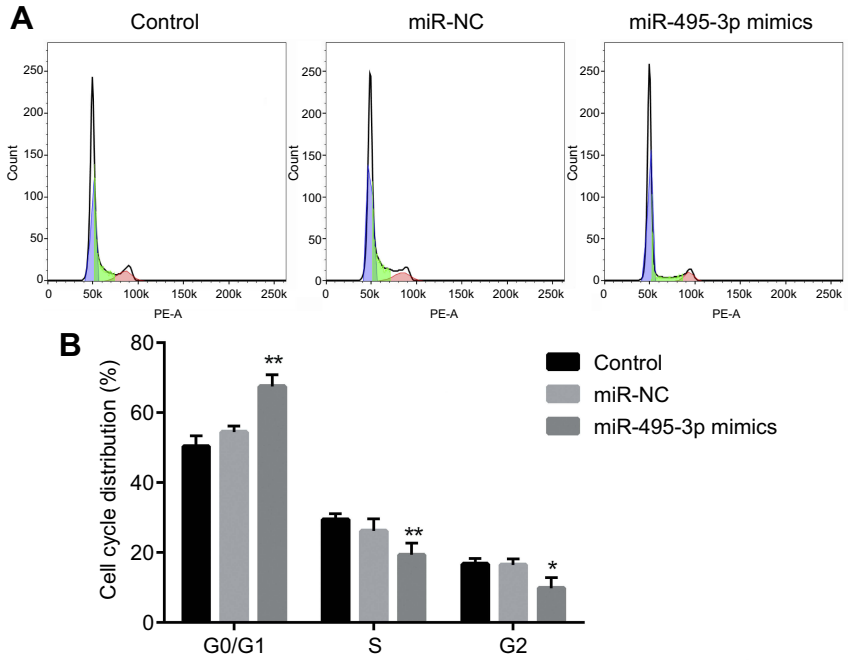

Figure 4 Overexpression of miR-495-3p induced cell cycle arrest. (**A**) Cell cycle was measured by flow cytometry analysis. (**B**) The cell cycle distribution was quantified. **P*<0.05, ***P*<0.01 vs miR-NC.

whereas cells in the S phase and G2 phase were markedly decreased, which indicated that there was cell cycle arrest. At the same time, the expression of cell cycle-related proteins, including p-Rb, CDK4, CDK6, Cyclin D1 and Cyclin A2, was down-regulated (Figure 5). However, apoptosis rate of the cells was increased following miR-495-3p overexpression compared with the miR-NC group (Figure 6A and B). In addition, the expression of apoptosis-related proteins was

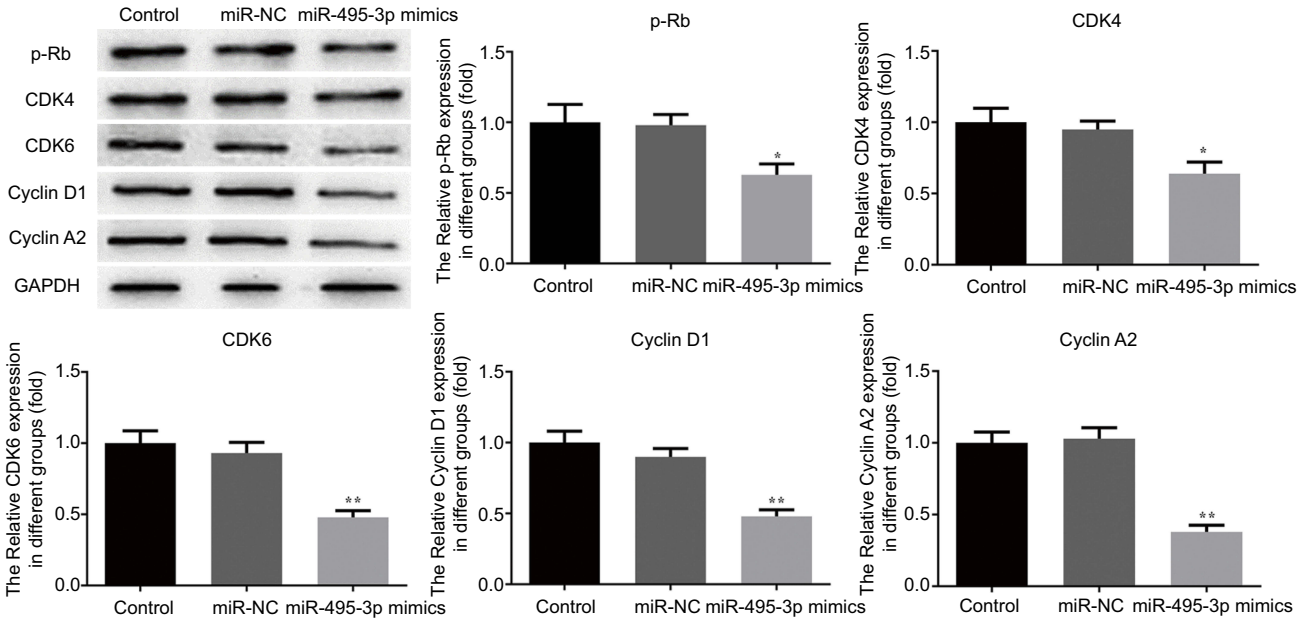

Figure 5 Overexpression of miR-495-3p affected the expression of cell cycle-related proteins. The expression levels of p-Rb, CDK4, CDK6, CyclinD1 and CyclinA2 were measured by western blotting. *P<0.05, **P<0.01 vs miR-NC.

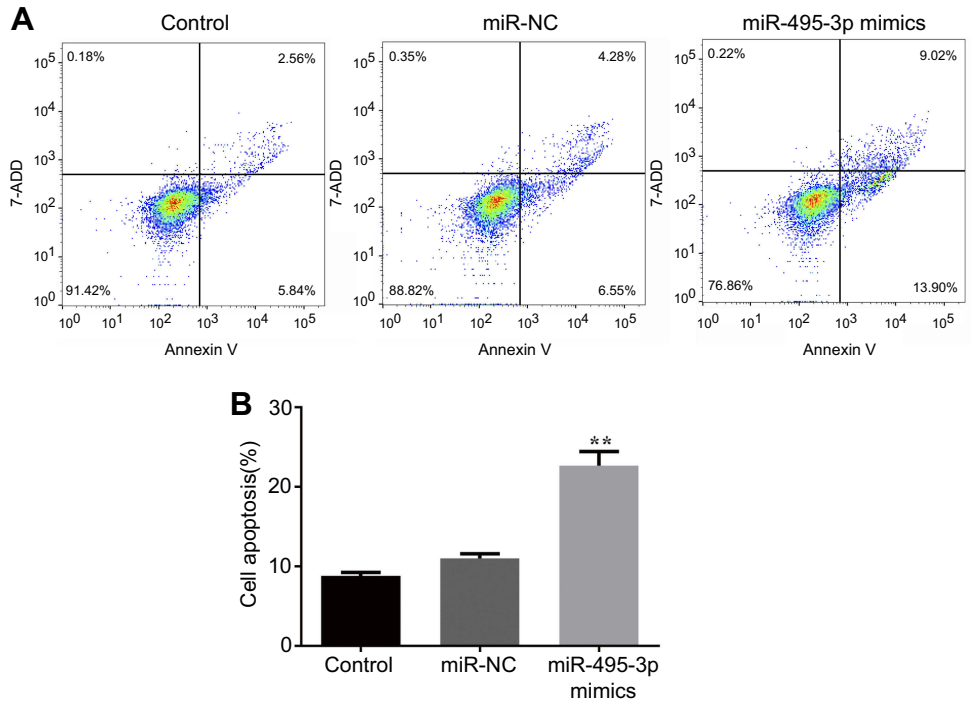

Figure 6 Overexpression of miR-495-3p promoted apoptosis in MG-63 cells. (**A**) Cell apoptosis was assessed by flow cytometry analysis. (**B**) Cell apoptosis was quantified. **P<0.01 vs miR-NC.

measured. From the results in Figure 7, we found that the expression of Bcl-2 was downregulated, whereas Bax and cleaved-Caspase-3 were upregulated significantly. These data suggested that overexpression of miR-495-3p induced cell cycle arrest, as well as promoting apoptosis in OS cells.

CTRP3 was a direct target of miR-495-3p

The western blot and RT-qPCR data indicated that the CTRP3 level was decreased following transfection with miR-495-3p mimics (Figure 8A and B). The function of miRNAs mainly depends on their target genes. Using the

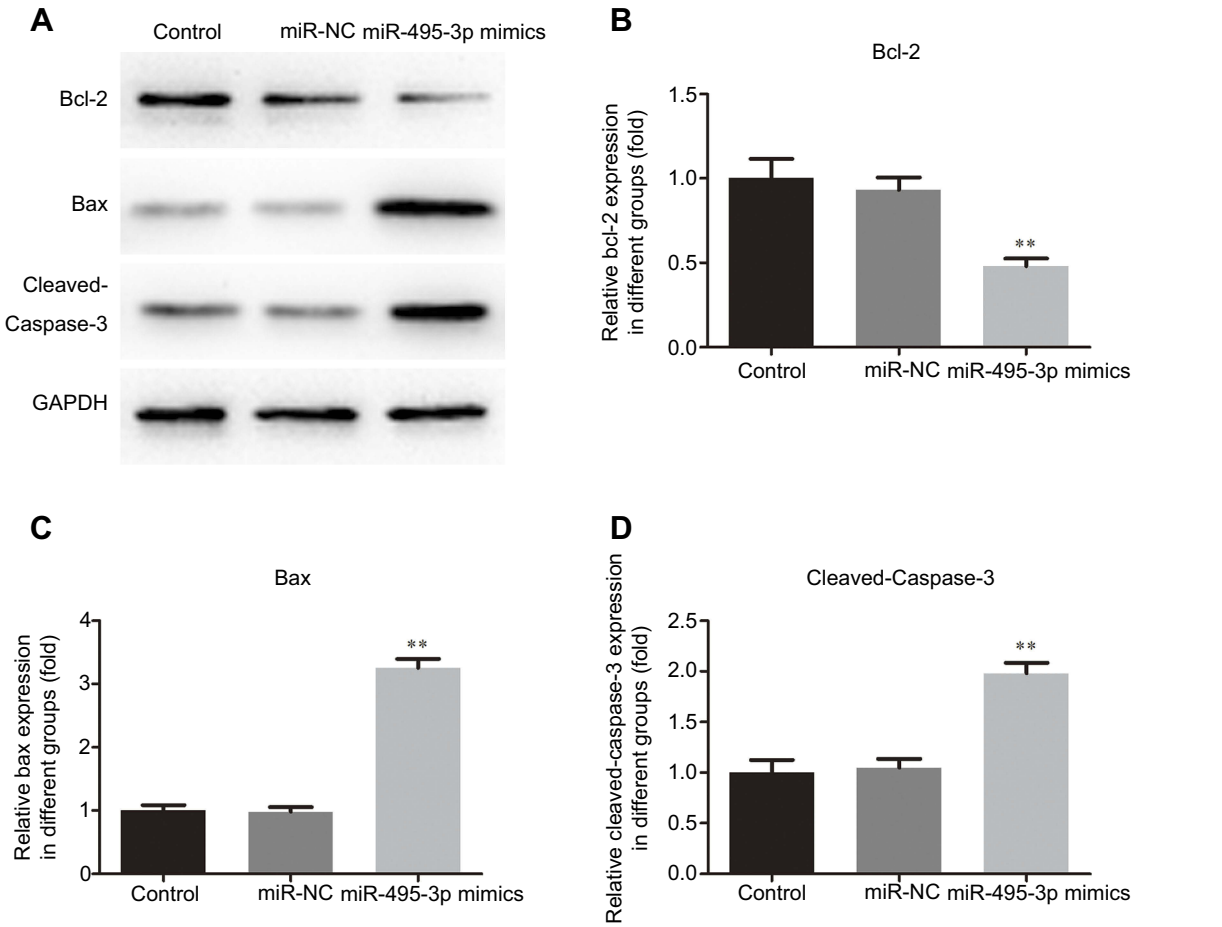

Figure 7 Overexpression of miR-495-3p affected the expression of apoptosis-related proteins. The expression levels of Bcl-2, Bax and cleaved-Caspase-3 were measured by western blotting. $^{**}P<0.01$ vs miR-NC.

bioinformatics database (www.TargetScan.org), we found that CTRP3 was a potential target of miR-495-3p (Figure 8C). To investigate whether CTRP3 was a direct target of miR-495-3p, the dual luciferase assay was performed. Co-transfection with miR-495-3p mimics and CTRP3 wild type 3′-UTR resulted in reduced luciferase activity, but miR-495-3p mimics did not change the luciferase activity in the CRTP3 mutant 3′-UTR group (Figure 8D). These results indicated that CTRP3 was a direct target of miR-495-3p.

Overexpression of miR-495-3p exerted a protective effect on OS in vivo

To evaluate the effect of miR-495-3p on OS in vivo, the xenograft OS model was established successfully. We measured the tumor weight and volume after transfection with miR-495-3p mimics. As shown in Figure 9, the tumor weight and volume were decreased notably in the miR-495-3p mimics group compared with the miR-NC group. Additionally, the mRNA and protein expression of CTRP3 was reduced after miR-495-3p overexpression in the tumor tissues of the xenograft OS model (Figure 10). The above results denoted that miR-495-3p exerted a protective effect on OS in vivo.

Discussion

OS is the most common primary bone malignancy, which threatens human health due to its low survival rate. Despite the rapid development of OS therapies, numerous patients continue to suffer from local relapses or distant metastasis following surgery and intensive chemotherapy.[20] Hence, there is an urgent need to develop novel and effective therapeutic strategies for OS. Mounting evidence demonstrated that miRNAs play a significant role in the progression of cancer.[21,22] The function of miRNAs largely depends on controlling their downstream targets. With the aim of unraveling the precise mechanism of OS, the tumor-suppressing role of

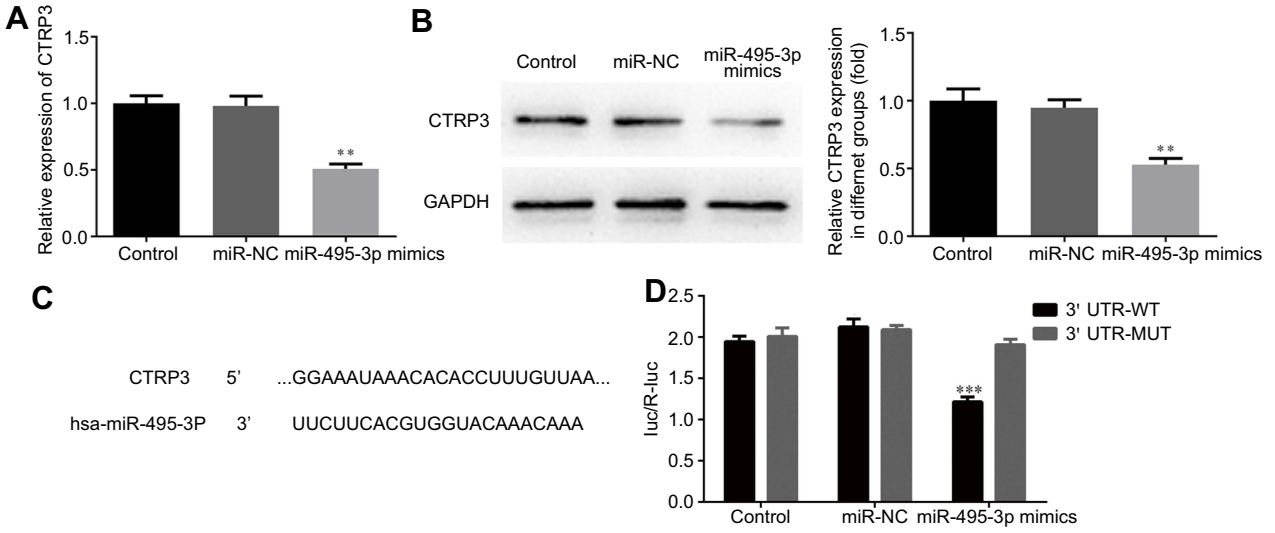

Figure 8 CTRP3 is a target gene of miR-495-3p. The expression level of CTRP3 was measured by RT-qPCR (**A**) and western blotting (**B**) after overexpression of miR-495-3p. ***P*<0.01 vs miR-NC. (**C**) Predicted miR-495-3p target sequence in the 3′-UTR of CTRP3. (**D**) The relative luciferase activity was measured by luciferase reporter assay. ****P*<0.001 vs 3′ UTR-WT.

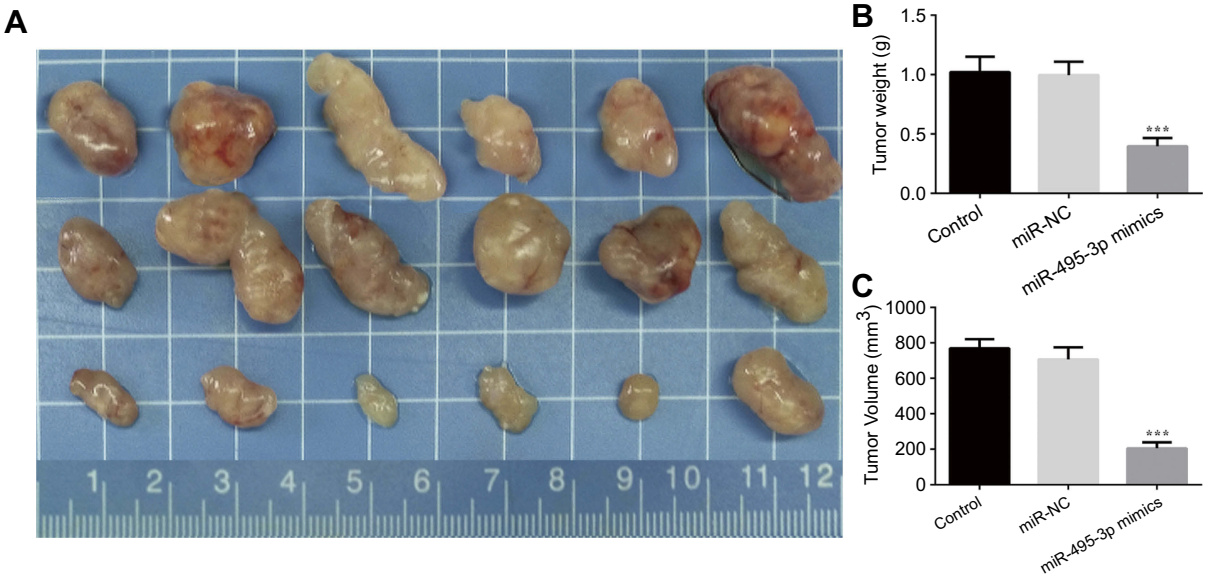

Figure 9 (**A**) Representative photographs of the osteosarcoma tumor mice after overexpression of miR-495-3p. Tumor weight (**B**) and tumor volume was quantified. ****P*<0.001 vs miR-NC.

miR-495-3p in OS was investigated for the first time, to the best of our knowledge, in the present study. In our study, the expression of miR-495-3p in OS tissues and cell lines was decreased and miR-495-3p overexpression suppressed the proliferation, migration and invasion of OS cells by down-regulating the expression of CTRP3, which was a direct target of miR-495-3p. Importantly, the experimental results in vivo were in accordance with it. These findings represented the anti-cancer effect of miR-495-3p in OS.

Accumulating evidence shows that miR-495-39p is involved in the formation of many human cancers. The previous study supports the idea that miR-495-3p is an important regulator of multidrug resistance by modulating the GRP78/mTOR axis in gastric cancer.[23] Emerging evidence

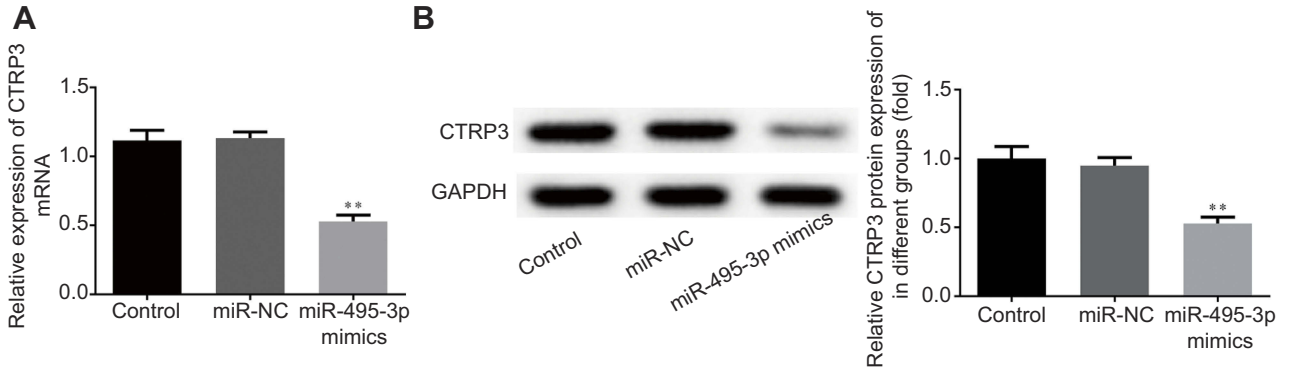

Figure 10 The expression level of CTRP3 was measured by reverse transcription-quantitative PCR (**A**) and western blotting (**B**) in xenograft osteosarcoma mice after overexpression of miR-495-3p. $^{**}P<0.01$ vs miR-NC.

demonstrates that miR-495-3p has the strongest link with esophageal squamous cell carcinoma.[24] In clear cell renal cell carcinoma, miR-495-3p has a suppressive effect on the proliferation and invasion of cancer cells.[12] miR-495-3p downregulation has been identified in human cancers, which was in agreement with our results in OS. However, to the best of our knowledge, there has been no investigation about the role of miR-495-3p in proliferation, migration and invasion in OS cells. To test the biological function of this miRNA, miR-495-3p overexpression was employed to conduct further research in an OS cell line by transfecting with miR-495-3p mimics. The results confirmed that overexpression of miR-495-3p suppressed the proliferation, migration and invasion, and promoted the apoptosis of OS cells. At the same time, the expression levels of cell cycle-related proteins, including p-Rb, CDK4, CDK6, CyclinD1 and CyclinA2, were decreased notably in the miR-495-3p mimics group, whereas the anti-apoptosis protein Bcl-2 was increased accompanied by a reduction in the expression of Bax and cleaved-Caspase-3.

To clarify the underlying mechanism of action of miR-495-3p in OS, potential target genes were identified using target prediction tools. CTRP3 was a direct target of miR-495-3p, which was verified by RT-qPCR and dual luciferase assays. CTRP, as a new adipokine, exerts crucial influences on protection against myocardial dysfunction, hepatic triglyceride accumulation and gestational diabetes mellitus.[15,25,26] Importantly, it has been well documented that CTRP3 plays an important role in bone metabolism via negative regulation of osteoclastogenesis.[18] In addition, a previous study reported that the serum CTRP3 level is associated with osteoporosis in postmenopausal women.[19] Moreover, we found that overexpression of miR-495-3p led to a significant reduction in CTRP3 protein and mRNA levels. Furthermore, the suppressive effects of miR-495-3p on the proliferation, migration and invasion of OS were obviously reduced by enforced CTRP3 expression. To confirm the effect of miR-495-3p in vivo, a xenograft OS model was generated for the research. The tumor weight and volume after transfection with miR-495-3p mimics were attenuated significantly. Importantly, the protein and mRNA expression levels of CTRP3 were lowered in the miR-495-3p mimics group, which was in accordance with the research in vitro. These findings indicated that the anti-cancer function of miR-495-3p in OS was at least partially mediated through targeting of CTRP3.

In conclusion, the present study demonstrated that the expression of miR-495-3p was significantly downregulated in vitro and in vivo in OS, and miR-495-3p overexpression suppressed cell proliferation, migration and invasion, potentially by targeting CTRP3. These findings indicated a novel tumor suppressive role of miR-495-3p in the development of OS, and may provide a potential therapeutic target for OS treatment.

Acknowledgments

The authors acknowledge all the participants and participating institutes for experimental and technical support in this study. The present study was supported by the Natural Science Foundation of China (81702667).

Disclosure

The authors report no conflicts of interest in this work.

References

1. Ji F, Zhang H, Wang Y, et al. MicroRNA-133a, downregulated in osteosarcoma, suppresses proliferation and promotes apoptosis by targeting Bcl-xL and Mcl-1. *Bone*. 2013;56:220–226. doi:10.1016/j.bone.2013.05.020

2. Yang J, Zhang W. New molecular insights into osteosarcoma targeted therapy. *Curr Opin Oncol*. 2013;25:398–406. doi:10.1097/CCO.0b013e3283622c1b
3. Gougelet A, Pissaloux D, Besse A, et al. Micro-RNA profiles in osteosarcoma as a predictive tool for ifosfamide response. *Int J Cancer*. 2011;129:680–690. doi:10.1002/ijc.25715
4. Harrison DJ, Geller DS, Gill JD, et al. Current and future therapeutic approaches for osteosarcoma. *Expert Rev Anticancer Ther*. 2018;18:39–50. doi:10.1080/14737140.2018.1413939
5. Irwandi RA, Vacharaksa A. The role of microRNA in periodontal tissue: A review of the literature. *Arch Oral Biol*. 2016;72:66–74. doi:10.1016/j.archoralbio.2016.08.014
6. Ameres SL, Zamore PD. Diversifying microRNA sequence and function. *Nat Rev Mol Cell Biol*. 2013;14:475–488. doi:10.1038/nrm3611
7. Ahmadzada T, Reid G, McKenzie DR. Fundamentals of siRNA and miRNA therapeutics and a review of targeted nanoparticle delivery systems in breast cancer. *Biophys Rev*. 2018;10:69–86. doi:10.1007/s12551-017-0392-1
8. Wang QX, Zhu YQ, Zhang H, et al. Altered MiRNA expression in gastric cancer: a systematic review and meta-analysis. *Cell Physiol Biochem*. 2015;35:933–944. doi:10.1159/000369750
9. Lodewijk L, Prins AM, Kist JW, et al. The value of miRNA in diagnosing thyroid cancer: a systematic review. *Cancer Biomark*. 2012;11:229–238. doi:10.3233/CBM-2012-0273
10. Liu Y, Li Y, Liu J, et al.MicroRNA-132 inhibits cell growth and metastasis in osteosarcoma cell lines possibly by targeting Sox4. *Int J Oncol*. 2015;(47):1672–1684. doi:10.3892/ijo.2015.3147.
11. Cheng DD, Yu T, Hu T, et al. MiR-542-5p is a negative prognostic factor and promotes osteosarcoma tumorigenesis by targeting HUWE1. *Oncotarget*. 2015;6:42761–42772. doi:10.18632/oncotarget.6199
12. Wang LN, Zhu XQ, Song XS, et al. Long noncoding RNA lung cancer associated transcript 1 promotes proliferation and invasion of clear cell renal cell carcinoma cells by negatively regulating miR-495-3p. *J Cell Biochem*. 2018;119:7599–7609. doi:10.1002/jcb.27099
13. Eun JW, Kim HS, Shen Q, et al. MicroRNA-495-3p functions as a tumor suppressor by regulating multiple epigenetic modifiers in gastric carcinogenesis. *J Pathol*. 2018;244:107–119. doi:10.1002/path.4994
14. Liu P, Shen JK, Hornicek FJ, et al. Wnt inhibitory factor 1 (WIF1) methylation and its association with clinical prognosis in patients with chondrosarcoma. *Sci Rep*. 2017;7:1580. doi:10.1038/s41598-017-01763-8
15. Li JY, Wu GM, Hou Z, et al. Expression of C1q/TNF-related protein-3 (CTRP3) in serum of patients with gestational diabetes mellitus and its relationship with insulin resistance. *Eur Rev Med Pharmacol Sci*. 2017;21:5702–5710. doi:10.26355/eurrev_201712_14016
16. Peterson JM, Wei Z, Wong GW. C1q/TNF-related protein-3 (CTRP3), a novel adipokine that regulates hepatic glucose output. *J Biol Chem*. 2010;285:39691–39701. doi:10.1074/jbc.M110.180695
17. Schmid A, Kopp A, Hanses F, et al. C1q/TNF-related protein-3 (CTRP-3) attenuates lipopolysaccharide (LPS)-induced systemic inflammation and adipose tissue Erk-1/-2 phosphorylation in mice in vivo. *Biochem Biophys Res Commun*. 2014;452:8–13. doi:10.1016/j.bbrc.2014.06.054
18. Kim JY, Min JY, Baek JM, et al. CTRP3 acts as a negative regulator of osteoclastogenesis through AMPK-c-Fos-NFATc1 signaling in vitro and RANKL-induced calvarial bone destruction in vivo. *Bone*. 2015;79:242–251. doi:10.1016/j.bone.2015.06.011
19. Xu ZH, Zhang X, Xie H, et al. Serum CTRP3 level is associated with osteoporosis in postmenopausal women. *Exp Clin Endocrinol Diabetes*. 2018;126(9):559–563.
20. Ottaviani G, Jaffe N. The etiology of osteosarcoma. *Cancer Treat Res*. 2009;152:15–32. doi:10.1007/978-1-4419-0284-9_2
21. Osada H, Takahashi T. MicroRNAs in biological processes and carcinogenesis. *Carcinogenesis*. 2007;28:2–12. doi:10.1093/carcin/bgl185
22. Zhang B, Pan X, Cobb GP, et al. microRNAs as oncogenes and tumor suppressors. *Dev Biol*. 2007;302:1–12. doi:10.1016/j.ydbio.2006.08.028
23. Chen S, Wu J, Jiao K, et al. MicroRNA-495-3p inhibits multidrug resistance by modulating autophagy through GRP78/mTOR axis in gastric cancer. *Cell Death Dis*. 2018;9:1070. doi:10.1038/s41419-018-1111-y
24. Kubota Y, Kaneko K, Konishi K, et al. The onset of angiogenesis in a multistep process of esophageal squamous cell carcinoma. *Front Biosci (Landmark Ed)*. 2009;14:3872–3878.
25. Wei WY, Ma ZG, Zhang N. Overexpression of CTRP3 protects against sepsis-induced myocardial dysfunction in mice. *Mol Cell Endocrinol*. 2018;476:27–36. doi:10.1016/j.mce.2018.04.006
26. Trogen G, Bacon J, Li Y. Transgenic overexpression of CTRP3 prevents alcohol-induced hepatic triglyceride accumulation. *Am J Physiol Endocrinol Metab*. 2018;315:E949–E960. doi:10.1152/ajpendo.00050.2018